Localization of a Micro AUV with Dynamic Trilateration Using Low-power Packet Radio RSSI

Thanathorn Phoka[1], Kritsana Kumphet[2], and Wansuree Massagram[3]

ABSTRACT: Communication radio-based localization is demonstrated in this work. The proposed solution was formulated and derived for both stationary and linearly drifting objects and can provide positioning data in GNSS-denied operations. Linear curve fitting on experimental data for radio-distance mapping with range calculation shows a real-world power—range relationship in both terrestrial and marine environments. The use of packet radio equipment on a secondary basis for localization may allow a reduction in requirements for high precision or task-specific hardware in the future.

Keywords: : Localization, Trilateration, GNSS-denied Environments, RSSI, XBee, 802.15, AUV, SeaGlide

DOI: 10.37936/ecti-cit.2021152.239947

Article history: received February 29, 2020; revised April 14, 2020; accepted April 22, 2020; available online April 22, 2021

1. INTRODUCTION

The deployment of man-portable autonomous underwater vehicles (AUVs) has become an integral part of oceanographic study. A review of the global inventory of AUVs [1], including gliders for marine surveying, reveals that many AUVs are available off-the-shelf. Some are propeller-driven, others are buoyancy-driven. The propeller-driven AUV basic configuration, as discussed by Madureira et al. [2], typically weighs more than 15 kg, with the standard length and diameter of 1.2 m and 0.15 m, respectively. These AUVs are capable of gathering data from the water column such as conductivity-temperature-depth (CTD), turbidity, pH level, and dissolved oxygen. They are also equipped with an acoustic modem, GSM, and WLAN for communication. The main advantage of the propeller-driven AUVs is their maneuverability.

A different type of AUV glides through the water by changing buoyancy. These "gliders" are energy efficient. This makes them attractive for long-term and long-range oceanographic survey. However, the directional trajectory of these AUVs is affected by the water current. This presents benefits and drawbacks. If the survey needs to be performed along the path of a water current, the buoyancy-driven AUVs can glide along effortlessly with the current. However, for maneuvering in tight confines or strong currents, other options may be needed.

The most prominent buoyancy-driven AUV is the Kongsberg's Seaglider [3]. It is a commercially available underwater vehicle suitable for long-range oceanographic survey. A CTD package is available for basic data collection. More sensors can be added to the Seaglider for specific commercial and advanced marine applications. Vertical motion is accomplished through changes in the vehicle buoyancy, adjusting its effective density. Steering is controlled by altering in the center of mass, accomplished by shifting the battery packs. Nonetheless, these systems are large, heavy, and expensive. These factors discourage their use in a smaller body of water such as freshwater lakes or irrigation canals. Furthermore, the prices make it difficult for smaller organizations or those with lower funding levels to procure and operate them. Similar to other commercially available AUVs, these gliders

[1,2,3]Department of Computer Science and Information Technology, Naresuan University, Phitsanulok, 65000, THAILAND., E-mail: thanathornp@nu.ac.th and wansureem@nu.ac.th

[1]Research Center for Academic Excellence in Nonlinear Analysis and Optimization Faculty of Science, Naresuan University, Phitsanulok, 65000, THAILAND., E-mail: thanathornp@nu.ac.th

[3]Corresponding author: wansureem@nu.ac.th

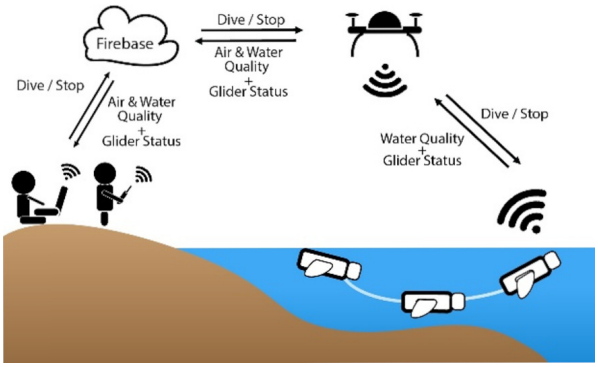

Fig.1: *Block diagram for system described by Banlue et al. [5]. The air and water quality measurements are collected simultaneously on an aerial vehicle and a modified SeaGlide, then sent to a Firebase instance for storage. The SeaGlide mission activity can be controlled from a web application.*

come with proprietary hardware and software which are difficult to modify. This limits researchers' ability to customize the vehicle behaviour or alter other aspects of the surveys.

The main challenge for the micro AUV producers is to miniaturize the gliders to create a small enough system that allows scientists, government officials, or those who want to check the water quality in small areas to do their work more easily at a significantly lower cost. The buoyancy-driven technique can be applied to a micro AUV.

SeaGlide, popularized by Robonotation, is a miniature AUV. The body of the vessel is made out of a 700-ml water bottle. The AUV itself does not have a propeller and only uses minimal energy to "glide" in and out of the water. A programmable Arduino microcontroller regulates the vehicles buoyancy and pitch. By pulling the plunger back and forth with a servo motor, the SeaGlide adjusts its buoyancy using available water. This buoyancy engine enables the water gliding saw-tooth motion. The SeaGlide moves forward in a dive by taking in water. This change in buoyancy and pitch causes it to sink and tilt down in the water. For the rise cycle, the glider expels water, pitches up, and rises towards the surface. The underwater SeaGlide robotic program has been proven to be an effective interdisciplinary approach to promote STEM education [4].

The Arduino in the SeaGlide allows more capability than locomotion control. The microcontroller can be used to receive and transfer measurement data. The adaptation of this micro AUV with additional sensors and communications has demonstrated the SeaGlide's potential for operational use as a part of an air and water quality survey study [5]. The SeaGlider is intended as a small and inexpensive AUV for use in water quality assessment in lakes and bodies of freshwater and littoral areas too confined for effective use of full-size underwater gliders. In a previous project [5], upon which this work builds, environmental measurements are collected both above and below the water surface. The aerial vehicle carries a payload for air quality measurements and also acts as a flying modem for the AUV, as seen in Fig. 1.

Fig.2: *A modified SeaGlide, equipped with a pH sensor, a temperature sensor, a GPS receiver, an XBee module, and a microcontroller, in a small test pool.*

Wireless communication is provided by a low-power 802.15.4 packet radio. The SeaGlide, equipped with a pH sensor and a temperature sensor, collects water quality measurements. The array of data, which includes the pH level, temperature, and location coordinates, is sent to the hovering drone via an XBee Pro S2C module. The system design integrates sensing, data caching, and wireless telemetry download to a nearby mobile device when the glider surfaces. Data is automatically uploaded to Firebase online storage, from which it can be accessed via Internet connectivity.

When the modified SeaGlide, seen in Fig. 2, is at the water surface, its location can be tracked using a global navigation satellite system (GNSS) module inside the fuselage. Diving and resurfacing during normal operation presents challenges for the GNSS tracking. The SeaGlide's almanacs and ephemerides, (ii) wait for a GNSS fix before diving, and (iii) ensure that the GNSS antenna has a clear view of the sky, without water shielding the path to the GNSS space vehicles when resurfacing.

GPS tracking of the SeaGlide might be improved through these operational constraints: (i) wait for GNSS receiver to acquire a position fix and also update the almanacs and ephemerides, (ii) wait for a GNSS fix before diving, and (iii) ensure that the GNSS antenna has a clear view of the sky, without water shielding the path to the GNSS space vehicles when resurfacing.

Despite taking these precautionary measures, many small, low cost, low-quality GNSS modules still suffer from signal loss due to this uncommon operating environment. An expedition for air and water environmental survey using Banlue's setup [5] was prepared. During the experiments, the GNSS tracking

was found to be inaccurate up to 50% of the time, especially during less than favourable weather. The SeaGlide often had to wait at least five minutes in order to acquire a position fix. During missions, it acquired an updated position fix upon resurfacing 80% of the time. Since the GNSS position fixes were not always available and not consistently accurate, an alternative positioning system can improve the mission capability of the SeaGlide.

The positioning system proposed here uses the strength of received radio frequency (RF) communication signals to estimate location by replicating the system used by satellite based navigation systems. Wireless sensor networks have been shown to be an effective tool for localization in various real-life applications [6]–[9]. In this paper, a new localization technique based on trilateration is formulated. The localization of a movable or stationary object from its range measurements to three known points is known as "trilateration". This technique is commonly applied to robot localization, kinematics, aeronautics, crystallography, and computer graphics [10]. GNSS position fixes are also determined using trilateration (or more precisely, multilateration) using receiver measured ranges to multiple satellites. Unlike traditional trilateration, where the known points are stationary and/or presented simultaneously, this study presents a dynamic triangulation method using movable known points (positions of a flying drone) to find the location of a movable object (a SeaGlide). The drone and the SeaGlide have an established wireless communication link via XBee radio, which can be also for localization. An analytical model of trilateration using XBee radio received signal strength indicators (RSSI) is derived. The performance of the algorithm was evaluated. The localization of a micro AUV with dynamic trilateration using XBee radio RSSI could prove its potential to other applications that require finding the position of a movable object in a sensor network.

The organization of this paper is as follows. The background theory of the proposed localization is described in Section 2. Sections 3 and 4 depict the experimental procedures and their results respectively. A discussion of the research's significance is presented in Section 5. The conclusion and directions for future work for this study are summarized in Section 6.

2. METHODOLOGY

The proposed solution for the localization problem involves three aspects: trilateration, drifted positions, and distance estimation using RSSI. The background theory and the proposed solution are explained in the following subsections.

2.1 Trilateration

When the GPS is not accurate or available, other positioning systems can be accessed to determine the location of an object. Localization can be achieved via wireless sensor networks using received signal strength indicators (RSSI) from two common approaches: (i) fingerprints, and (ii) trilateration. The fingerprinting approach needs intensive computational power due to its training and recalibration requirements. This study selected a positioning system based on RSSIs and trilateration using XBee technology [9], [11], [12].

Trilateration is a central component to locate a position within networks of sensors where range measurement is achievable. Determining the location of an object with trilateration uses distances between the object and three spatially-separated known sites. Localization using trilateration [10] is normally expressed as the problem of locating the coordinate (x, y) where three circles intersect with the following quadratic equations:

$$\begin{aligned}(x-x_1)^2+(y-y_1)^2&=r_1^2\\(x-x_2)^2+(y-y_2)^2&=r_2^2\\(x-x_3)^2+(y-y_3)^2&=r_3^2\end{aligned} \tag{1}$$

where $\boldsymbol{ci=(xi,yi)}$ are the coordinates of the known sites and $\boldsymbol{r_i}$ is the distance between the known sites and the object of interest at $(\boldsymbol{x,y})$. The quadratic equations in (1) can be expanded as follows:

$$\begin{aligned}(x^2-2xx_1)^2+x_1^2+y^2-2yy_1+y_1^2&=r_1^2\\(x^2-2xx_2)^2+x_2^2+y^2-2yy_2+y_2^2&=r_2^2\\(x^2-2xx_3)^2+x_3^2+y^2-2yy_3+y_3^2&=r_3^2\end{aligned} \tag{2}$$

Subtracting equations in (2) from each other results in:

$$(-2x_1+2x_2)x+(-2y_1+2y_2)y=r_1^2-r_2^2-x_1^2+x_2^2-y_1^2+y_2^2$$

and

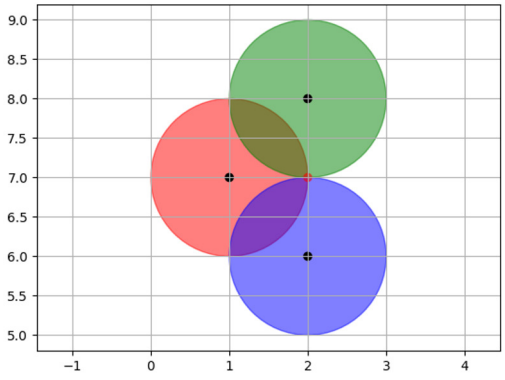

Fig.3: *An example of a trilateration problem with the coordinates of the known sites c_i at (1, 7),(2, 8) and (2, 6) to locate the object at one unit distance from all three sites. The solution for this problem can be found at (2, 7).*

$$(-2x_1+2x_2)x+(-2y_1+2y_2)y=r_1^2-r_2^2-x_1^2+x_2^2-y_1^2+y_2^2$$

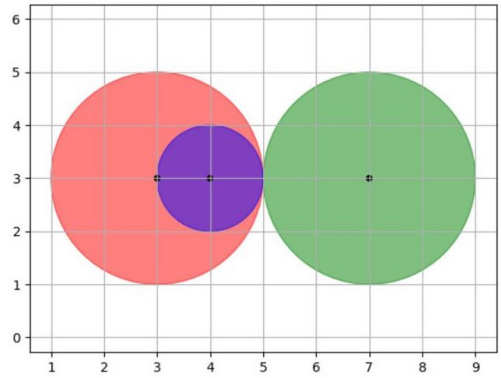

Fig.4: *An example of a trilateration singularity with the coordinates c_i of the known sites, (3, 3),(7, 3) and (4, 3), which are aligned on the y-axis. The solution for this problem cannot be found due to division by zero.*

These can be written using two equations with two unknowns as follows:

$$\begin{aligned} Ax + By &= C \\ Dx + Ey &= F \end{aligned} \tag{3}$$

This leads to the numerically solvable solution:

$$\begin{aligned} x &= \frac{CE - FB}{EA - BD} \\ y &= \frac{CD - AF}{BD - AE} \end{aligned} \tag{4}$$

An example of a traditional trilateration problem is illustrated in Fig. 3. The problem contains three known sites: (1, 7), (2, 6) and (2, 8) with one unit radius from all three points. When solving for the simplified form of trilateration in (4), the coordinate of the object of interest ($\boldsymbol{x,y}$) becomes (2, 7)

However, localization using trilateration does not always yield a solution despite the existence of an intersection of the three known sites. A case of trilateration singularity occurs when the three sensors are aligned, as seen in Fig. 4, which results in division by zero in (4). In such cases, $\boldsymbol{AE=BD}$.

Trilateration using XBee RSSI can be applied to the particular GPS tracking accuracy problem where the receiver cannot acquire the location coordinates under certain conditions. The drone can be utilized to obtain the known positions, $\boldsymbol{c_i}$, by flying to and hovering at three predetermined points. The drone's onboard GPS receiver can provide accurate coordinates ($\boldsymbol{x_i}, \boldsymbol{y_i}$). Since both drone and SeaGlide are equipped with XBee radios for communication, the distance measurements between the drone and the SeaGlide, $\boldsymbol{r_i}$, can be calculated from the RSSI.

To satisfy the conditions in equations (1) through (4), the SeaGlide must be stationary for the entire duration of the drone's flight path for the distance measurements. However, a floating object on the water surface does not naturally stay in one place. The SeaGlide will be drifting along the water current or with the wind direction. In an event where the position of the object of interest is not stationary, the following formulation is proposed to compensate for the object's change in position. The quadratic equations in (1) then become:

$$\begin{aligned} &(x-x_1)^2+(y-y_1)^2=r_1^2 \\ &(x-dx^{'}-x_2)^2+(y-dy^{'}-y_2)^2=r_2^2 \\ &(x-dx^{''}-x_2-x_3)^2+(y-dy^{''}-y_2-y_3)^2=r_2^3 \end{aligned} \tag{5}$$

where ($\boldsymbol{x\text{-}dx^{'}}, \boldsymbol{y\text{-}dy^{'}}$) and ($\boldsymbol{x\text{-}dx^{''}}, \boldsymbol{y\text{-}dy^{''}}$) are the first and second positions to which the floating object drifts, respectively. This can be numerically solved similarly to (4) for the two unknowns, $\boldsymbol{x}$ and $\boldsymbol{y}$.

The scenario for finding a location of a micro AUV with dynamic trilateration is illustrated in Fig. 5. The drone waits for the SeaGlide to resurface. When the SeaGlide rises to the surface of the water at (2, 7), the drone is hovering at (1, 7). The RSSI from the XBee communication between the two vehicles results in the range measurement, $\boldsymbol{r_1}$, of one unit apart. To complete the trilateration calculation, the drone then flies to the second predetermined point, (2, 8). By that time, the SeaGlide, experiencing wind and water currents, drifts to (4, 9), where $\boldsymbol{r_2}$ is measured. The drone completes its fly-through at (2, 6) where the SeaGlide now drifts to (7, 5). The original SeaGlide's coordinates at (2, 7) can be calculated from (5).

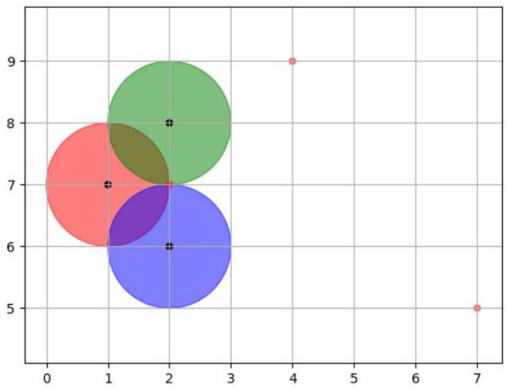

Fig.5: *An example of trilateration problem with a movable object of interest. The coordinates of the known sites, c_i, are at (1, 7),(2, 8) and (2, 6). The object of interest's first, second, and third positions are at (2, 7), (4, 9), and (7, 5) respectively.*

2.2 Drifted Position

The trajectory of a floating object on water depends on currents, wind directions, and the object's motion. The SeaGlide's drift trajectory and its eventual position can be computed using either one of two proposed methods:

1) Accelerometer: a widely-used sensor that measures acceleration in meters per second squared (m/s2) or in gravity force (g). To determine the position of an object with data from an accelerometer or a gyroscope, the double integration of acceleration is calculated. If the acceleration is a continuous function, position is calculated from double integral of the acceleration. If the acceleration is not a continuous function, the position is calculated part by part, then the parts are aggregated. For a constant acceleration, the displacement, $\boldsymbol{s}$, is commonly expressed as:

$$\boldsymbol{s}=\boldsymbol{ut}+\frac{\boldsymbol{1}}{\boldsymbol{2}}\boldsymbol{at}^{\boldsymbol{2}} \tag{6}$$

where $\boldsymbol{u}$ is the initial velocity, $\boldsymbol{t}$ is the elapsed time in seconds, and $\boldsymbol{a}$ is the acceleration. Sensory data fusion can be used to combine data collected by different sensors to obtain a more accurate position estimation with lower uncertainty compared to any independent measurement.

2) Drift model: a mathematical model that predicts the trajectory of a drifting object. Drifting prediction is an ongoing research topic with involvement from several stakeholders including marine search and rescue operators, maritime navigators, and oceanographers. Many studies rely on computers to simulate and forecast the drift trajectory using different proposed drift models [13]–[15]. These models include kinetic models of object shape and stochastic motion features, collected current measurements, analysis using hydrodynamic principles, and empirical parameterizations. Fundamentally, the position of a drifting object can be computed by integrating the total drift velocity, $\boldsymbol{V}_{\boldsymbol{drift}}$, of the object as given by

$$\boldsymbol{V}_{\boldsymbol{drift}} = \boldsymbol{V}_{\boldsymbol{curr}} + \boldsymbol{V}_{\boldsymbol{rel}} \tag{7}$$

where $\boldsymbol{V}_{\boldsymbol{curr}}$ represents the water current velocity and $\boldsymbol{V}_{\boldsymbol{rel}}$ represents the drift velocity of the object relative to the water [16].

The SeaGlide could be equipped with a commercially available inertial measurement unit (IMU) to provide vehicle attitude with heading relative to magnetic north. Theoretically, the data collected from the IMU's sensors would allow a computation of the current position by using a previously determined position, known as a fix, and advancing that position based upon known or estimated speeds over elapsed time and course. This method is often used in navigation and is known as "dead reckoning". However, this method typically suffers from accumulated error due to continuous integration which leads to an increasing difference between the calculated position and the actual location.

2.3 RSSI Range Estimation

Free-space path loss (FSPL) is a phenomenon in any wireless communication which explains the attenuation of radio energy between two antennas. The FSPL formula derives from the Friis transmission formula which states that in any radio system consisting of a transmitting antenna transmitting radio waves to a receiving antenna, the ratio of radio wave power received P_r to the power transmitted P_t is given by

$$\frac{P_r}{P_t} = D_r D_t \left(\frac{\lambda}{4\pi d}\right)^2 \tag{8}$$

where D_t is the directivity of the transmitting antenna, D_r is the directivity of the receiving antenna, λ is the signal wavelength, and d is the distance between the two antennas.

In wireless networks, the received signal strength indicator, or RSSI, is often used along with the percentage of received packets to measure the link reliability [17]. The RSSI is an indication of the RF energy detected at the receiving antenna. It is measured in dBm which is a unit of level of a power ratio in decibels (dB) with reference to 1 mW as given by

$$RSSI = 10\log\left(\frac{P_{RX}}{P_{REF}}\right) \tag{9}$$

where P_{RX} is the remaining power of a wave at the receiver in Watts and P_{REF} is a reference signal strength value, i.e. 1 mW.

The power at the receiving antenna, P_r, is proportional to the reciprocal of distance squared as shown in equation (8). P_{RX} in (9) depends on the path loss which is caused by fading, multipath, and FSPL [18]. As a result, the received signal strength indicator value is also inversely proportional to the squared distance as expressed by

$$RSSI \propto \log\left(\frac{1}{d^2}\right) \tag{10}$$

This explains the intuition that the farther away the transmitter is from the receiver, the weaker the strength of the signal at the receiving antenna is and thus the reliability of the communication declines.

To determine a function that could reasonably approximate distance as a function of RSSI value, (10) can be further simplified through logarithmic properties as

$$RSSI \propto \log d \tag{11}$$

or

$$RSSI \propto -ln(d) \tag{12}$$

which can be expressed in a linear equation as

$$RSSI \propto -aln(d) + b \tag{13}$$

where both a and b are its constant coefficients. These constants can be found through empirical experiments where the RSSIs are measured at a known distance.

3. EXPERIMENTAL SETUPS

The experiments were conducted on land and water to generate a function that best estimates the distance using the packet radio's received signal strength. The experimental procedures were conducted as follows.

To measure the packet radio RSSI, two XBee Pro S2C modules, which operate at 2.4 GHz, were used. This particular model of XBee radio has a range of up to 90 m indoors and 1.6 km outdoors. One XBee acts as a transmitter while the other is a receiver. The transmitting radio was mounted 0.8 m above the level plane as illustrated in Fig. 6.

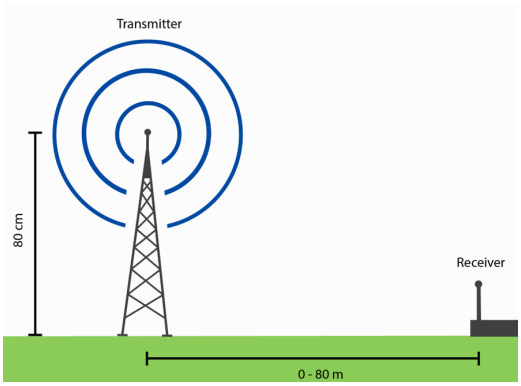

Fig.6: *The setup for RSSI measurements between two XBee Pro S2C packet radios with the transmitter 0.8 m above the ground. The longest distance between the two radios was 80 m.*

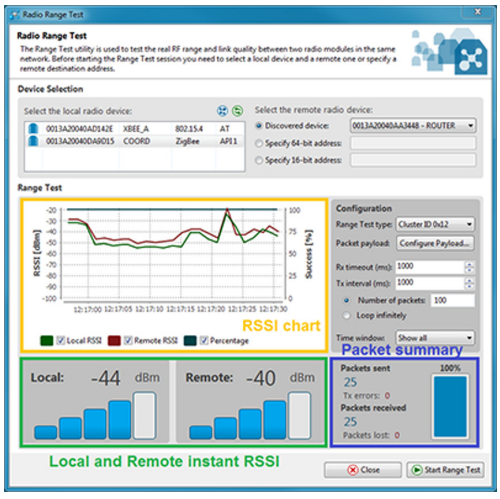

Fig.7: *XCTU configuration for the initial RSSI tests.*

As mentioned in Section 2.3, free space loss, multipath, and fading are the main factors causing signal path loss. For free space loss, even without other impairments, the signal still attenuates over distance. The multipath problem refers to the arrival of radio signals to a receiving antenna by more than one path with the direct and reflected signals not in phase. These arriving signals can cancel each other out, causing data loss at the receiver antenna. As for fading, the power of a wireless signal fluctuates depending on environmental effects. All these factors may affect the estimation of the range through RSSI. Thus, for this study, the differences in behaviour between on land and over the water RSSI were interesting given the applicable problem which needed to be overcome.

For the initial RSSI testing, XCTU, a multiplatform RF configuration application, was used [17]. Its graphical interface, shown in Fig. 7, allows the range test between two radio modules of the same network to be performed and the RSSI measurements to be recorded manually.

However, to estimate the coefficients for (13), fifty measurements were planned at each incremental distance for both land and water tests outdoors. XCTU was replaced by an Arduino program designed to read the RSSI values and record them in text files. Fifty RSSI values were obtained at a given distance away from the transmitter between 0 and 80 m with five meter resolution, resulting in 850 data points for the land and 850 data points for the water experiments. Fig. 8. shows the setup for the over water setting. The receiving antenna was mounted on a floating platform on the water.

4. RESULTS

The recorded values were plotted against the reciprocal distance, and a non-linear relationship was verified. Then linear regression was applied to the relationship between the RSSI values and the log of distance to generate the best linear fit for the data. The coefficients a and b in (13) were then obtained.

Fig.8: *The outdoor experimental setting for the RSSI measurement range test over water. The transmitter was mounted 0.8 m above the ground, while the receiver was mounted on a floating platform, seen as a white box at the top of this figure.*

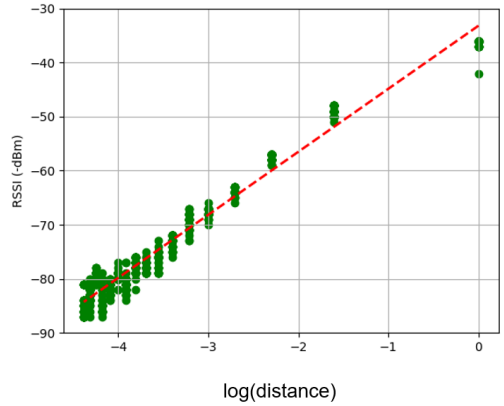

(a)

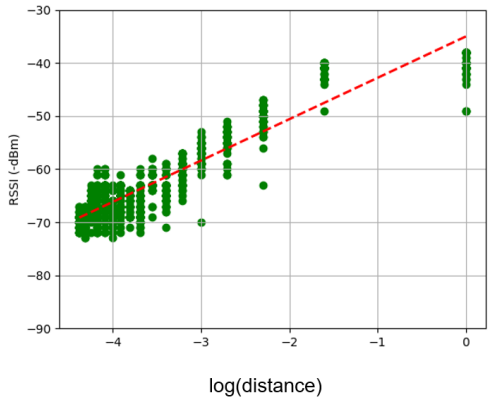

(b)

Fig.9: *The linear curve fit of the relation between RSSI in dBm and the log distance of (a) the data collected on land and (b) the data collected over the water.*

4.1 Linear Approximation

The measured RSSI values were plotted against the log of distance as shown in Fig. 9a for RSSI on land and Fig. 9b for RSSI over the water. The trend lines of the two figures are visibly different. The linear regression analysis provided an estimation of the equation (13) for each experiment. The linear regression coefficient, a, and the linear regression intercept, b, of (13) from the empirical experiments are shown in Table 1.

Table 1: *The linear regression coefficient, a, and the linear regression intercept, b of (13) from the empirical experiments.*

Experimental Setting	a	b
On land	-11.67	-33.19
Over water	-7.79	-35.01

For the land-based experiment, the linear curve fit gave the following relation between RSSI in dBm and distance in meters as the following equation:

$$RSSI_{land} = -11.67ln(d) - 33.19 \tag{14}$$

For the water-based experiment, the linear curve fit gave the following relation between RSSI and distance as the following equation:

$$RSSI_{water} = -7.79ln(d) - 35.01 \tag{15}$$

Equations (14) and (15) provide the formulas for the relationships between RSSI and distance for the packet radio XBee Pro S2C modules operating at 2.4 GHz on land and over the water respectively. To calculate for the distance between the transmitting and the receiving radios, (13) can be rewritten as

$$d = e^{\frac{b-RSSI}{a}} \tag{16}$$

which then can be used to find the distance measurements between the drone and the SeaGlider, r_i , in (5).

4.2 Accuracy Analysis

The distance between two XBee packet radios, which represents the distance measurement between the drone and the SeaGlider, could now be calculated from (16). Plots depicting this calculated distance and the measured distance can be seen in Fig. 10 for over-land and over-water communication links at multiple distances. In both situations, the differences between the calculated and measured distances increase at longer ranges. An interesting trend, especially for the over water measurements, is that the calculated distances are larger than the measured distances and most noticeably at longer ranges.

5. DISCUSSION

This study set out to discover an alternative solution for a localization of a small vessel using low-cost packet radio communication. A new localization technique for a movable object based on trilateration of RSSI signal strength is proposed, mathematically proven, and empirically tested to verify its feasibility. The proposed localization system can work in GNSS denied environments without any extra equipment to measure range. Such a system is suitable for the aerial-to-surface environmental survey where a small drone and a small AUV already have established wireless communication networks via a low-power packet radio.

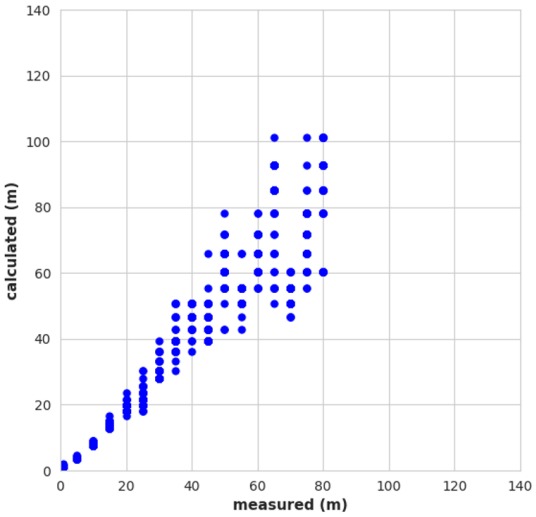

(a)

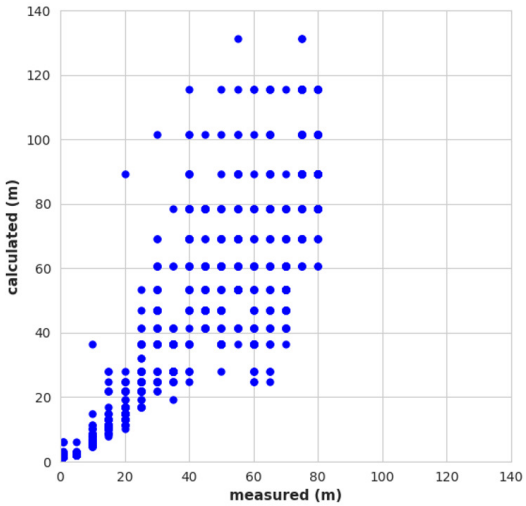

(b)

Fig.10: *Comparison of calculated and measured distance between transmitting and receiving radios above (a) land and (b) water.*

The radio transceivers used in these experiments provided RSSI at higher than preferable granularities, which limited the accuracy of calculated ranges. This may have also obscured some of the finer effects on received power and its relation to range.

Observed performance differed in terrestrial and aquatic environments. During these experiments, the vehicle was minimally disturbed by waves and currents. In other situations, waves and currents could reduce accuracy without compensation, which may be as simple as (i) an increase in measurements to determine location or (ii) radio transceivers able to provide more accurate range data.

In addition to the above recommendation for accuracy improvement, future study needs to address the global earth-centered, earth-fixed (ECEF) reference. The trilateration formulas, as seen in Section II, need three tuples in Cartesian coordinates, not spherical coordinates. Therefore, a displacement transform in the earth spherical coordinates into Cartesian coordinates is necessary. Future packet radios may incorporate improved diagnostics, e.g. finer grained RSSI, multiple-input and multiple-output (MIMO) direction finding, or direct determination of remote station range.

The results here illustrate the possibility of localization for GNSS-denied environments and could also be used in swarming networks of drones for fine position adjustments. This system provides a locally referenced position, not one directly depending on the ECEF reference, which could be useful for relative navigation.

6. CONCLUSION

This work provides mathematical formulations for the localization problem and an approach to calculate position information for two unmanned vehicles using packet radio equipment on a secondary basis. This technique could be used in GNSS-denied environments, with reduced requirements for high precision clocks or task-specific hardware. It could be useful to swarms of drones, assisting with fine positioning. Future packet radios may incorporate improved diagnostics. Such improvements would support an increase in accuracy without the need for dedicated rangefinders or high grade GNSS receivers.

ACKNOWLEDGMENT

The authors would like to thank to Dr. Noah Hafner and the members of Naresuan University Maker Club for their assistance.

References

[1] J. Hunt, “Global inventory of AUV and glider technology available for routine marine surveying,” 2013. [Online]. Available: `https://development.oceanbestpractices.net`

[2] L. Madureira, A. Sousa, J. Braga, P. Calado, P. Dias, R. Martins, J. Pinto, and J. Sousa, “The light autonomous underwater vehicle: Evolutions and networking,” in OCEANS-Bergen, 2013 MTS/IEEE. IEEE, 2013, pp. 1–6.

[3] C. C. Eriksen, T. J. Osse, R. D. Light, T. Wen, T. W. Lehman, P. L. Sabin, J. W. Ballard, and A. M. Chiodi, “Seaglider: A long-range autonomous underwater vehicle for oceanographic research,” *IEEE Journal of oceanic Engineering*, vol. 26, no. 4, pp. 424–436, 2001.

[4] S. Ziaeefard, B. R. Page, L. Knop, G. A. Ribeiro, M. Miller, M. Rastgaar, and N. Mahmoudian, “GUPPIE programa hands-on STEM learning experience for middle school students,” in *Frontiers in Education Conference (FIE). IEEE*, 2017, pp. 1–8.

[5] P. Banlue, S. Kiewbanyang, T. Phoka, and W. Massagram, “Aerial-tosurface communication

and data transferring system for environmental survey," in *2018 22nd International Computer Science and Engineering Conference (ICSEC). IEEE*, 2018, pp. 1–4.

[6] S. Shue, L. E. Johnson, and J. M. Conrad, "Utilization of XBee ZigBee modules and MATLAB for RSSI localization applications," in *SoutheastCon 2017. IEEE*, 2017, pp. 1–6.

[7] R. Shigeta, K. Suzuki, F. Okuya, and Y. Kawahara, "Trilaterationinspired sensor node position estimation for UAV-assisted microwave wireless power transfer," *SICE Journal of Control, Measurement, and System Integration*, vol. 10, no. 5, pp. 350–359, 2017.

[8] F. Sanfilippo and K. Y. Pettersen, "XBee positioning system with embedded haptic feedback for dangerous offshore operations: a preliminary study," in *OCEANS 2015-Genova. IEEE*, 2015, pp. 1–6.

[9] A. Heinemann, A. Gavriilidis, T. Sablik, C. Stahlschmidt, J. Velten, and A. Kummert, "RSSI-based real-time indoor positioning using zigbee technology for security applications," in *International Conference on Multimedia Communications, Services and Security*, Springer, 2014, pp. 83–95.

[10] F. Thomas and L. Ros, "Revisiting trilateration for robot localization," *IEEE Transactions on robotics*, vol. 21, no. 1, pp. 93–101, 2005.

[11] V. Honkavirta, T. Perala, S. Ali-Loytty, and R. Piche, "A comparative survey of WLAN location fingerprinting methods," in *2009 6th workshop on positioning, navigation and communication. IEEE*, 2009, pp. 243–251.

[12] A. Arya, P. Godlewski, and P. Melle, "Performance analysis of outdoor localization systems based on RSS fingerprinting," in *2009 6th International Symposium on Wireless Communication Systems. IEEE*, 2009, pp. 378–382.

[13] S.-z. Wang, H.-b. Nie, and C.-j. Shi, "A drifting trajectory prediction model based on object shape and stochastic motion features," *Journal of Hydrodynamics*, Ser. B, vol. 26, no. 6, pp. 951–959, 2015.

[14] J. Zhang, A. P. Teixeira, C. G. Soares, and X. Yan, "Probabilistic modelling of the drifting trajectory of an object under the effect of wind and current for maritime search and rescue," *Ocean Engineering*, vol. 129, pp. 253–264, 2017.

[15] Ø. Breivik, A. A. Allen, C. Maisondieu, and J. C. Roth, "Windinduced drift of objects at sea: The leeway field method," *Applied Ocean Research*, vol. 33, no. 2, pp. 100–109, 2011.

[16] B. Hackett, Ø. Breivik, and C. Wettre, "Forecasting the drift of objects and substances in the ocean," in *Ocean weather forecasting. Springer*, 2006, pp. 507–523.

[17] Digi International Inc., "Signal strength and the RSSI pin," 2019. [Online]. Available: `https://www.digi.com/resources/documentation/Digidocs/9000145613/concepts/c\_rssi\_pin\_and\_signal\_strength.htm`

[18] F. Ileri and M. Akar, "RSSI based position estimation in zigbee sensor networks," *WSEAS Recent Advances in Circuits, Systems, Signal Processing and Communications*, pp. 62–73, 2014.

Thanathorn Phoka is an assistant professor and assistant dean of Faculty of Science, Naresuan University. He received B.Eng, M.Eng, and Ph.D. in Computer Engineering from Chulalongkorn University in 2002, 2004, and 2011 respectively. His areas of expertise are computer vision and machine learning.

Kritsana Kumphet is a research assistant at NU Maker Club. He previously completed an internship at Knowledge Centric Co., Ltd. before receiving his B.S. in Computer Science from Naresuan University in May 2018. His interests are open-source hardware, EduTech, and maker culture.

Wansuree Massagram is a faculty member at Naresuan University. She graduated from Carnegie Mellon University with B.S. ('01) and M.S. ('02) in Electrical and Computer Engineering. She received a Ph.D. ('08) in Electrical Engineering from University of Hawaii. Her research topics include remote sensing and IoT.